Optica Applicata, Vol. XXIII, No. 2–3, 1993

Microscopic implementation of phase-stepping interferometry for dielectric surface evaluation in transmitted light

M. SOCHACKA*

Optical Laboratory, University of Santiago de Compostela, 15706 Santiago de Compostela, Galicia, Spain.

F. LE PREVOST

I. U. T. of Angers, Boulevard Lavoisier, Angers, France.

The phase-stepping technique with dia illumination is proposed to evaluate surface relief of a dielectric layer and the height of abrupt thickness steps. An easy implementation is described in a commercially available polarized light interference microscope. Experimental results are presented.

1. Introduction

Since its introduction by BRUNNING *et al.* [1] in 1974, the phase-stepping interferometry (PSI) has become one of the best, quickest and most elegant interferometric techniques. It has found applications in a great number of wavefront measuring devices for control, surface profiling, recognition of shape and deformation of optical elements, as well as measurement of vibration amplitudes and phases [2], [3]. Many modifications of the original algorithm have also been made (see review by CREATH [4] and an extensive bibliography herein) in order to improve the PSI accuracy and speed. The greatest advantage of PSI and related methods is that they can be easily implemented in automatic systems for quantitative phase retrieval.

Most PSI implementations use two-arm interferometers with a reference surface in one of them and a piezoelectric transducer (PZT) to introduce necessary phase changes by sample or reference translation. The use of other phase shifters, such as rotating polarizers, tilted glass plates and diffraction gratings, has also been widely considered [2], [4] and application of a Wollaston prism in phase-shifting moiré interferometry has been proposed [5].

The PSI has found applications in microinterferometry, too, being used in topography of highly polished reflecting surfaces [2], [5]–[8], [10]. They are based on different interferometer principles (Fizeau, Mireau, *etc.*) and the PZT is mostly used as a phase shifter. In one of such implementations it was proposed to evaluate

*On leave from Intitute of Applied Optics, ul. Kamionkowska 18, 03-805 Warszawa, Poland.

abrupt steps in reflecting surface [9]. The Nomarski DIC microscope was used to measure the roughness of highly polished reflecting surfaces, as reported by SHIMADA, SATO and YATAGAI [10].

In this paper, the microscopic implementation of the phase-stepping in transmitted light is described in a commercially available instrument, both for differential image shearing and for the total one. Those two configurations have different applications that depend on the object properties. Such applications can be the surface profiling of photoresist impressed patterns and thickness measurement of very thin optical coatings described in this work.

In the following sections, a short introduction to the theory of the phase-stepping interferometry is given, the experimental set-up described and the experiment results discussed.

2. Basics of the phase-stepping interferometry

The intensity distribution, as observed in the exit plane of any interferometer, can be generally described as

$$I = I_0 + I_C \cos[\Delta(x,y) - \Phi_B] \tag{1}$$

or, equivalently

$$I = I_0 + I_C \cos\Delta(x,y)\cos\Phi_B + I_C \sin\Delta(x,y)\sin\Phi_B \tag{2}$$

where I_0 is the background intensity, I_c is the interference pattern amplitude governing the image contrast, $\Delta(x,y)$ is the phase change introduced by an object investigated, and Φ_B is the bias (phase difference between the interfering wavefronts, a quantity characteristic of the instrument). When Φ_B is a constant, the observed field is a homogeneous one (in the absence of $\Delta(x,y)$). When Φ_B is a function of space coordinates, a fringe pattern appears that will be perturbed by the presence of the $\Delta(x,y)$ phase.

From formula (1) it follows that the intensity I in an interferogram is a periodic function of the bias Φ_B with 2π period, so it can be alternately represented by a Fourier series in terms of Φ_B. Taking into account only the constant and the first-order terms of such expansion and comparing them with formula (2) it follows that the ratio of the first-order coefficients a_1 and b_1 of the Fourier expansion gives the tangent of the phase change $\Delta(x,y)$.

To simplify the calculation of coefficients a_1 and b_1 the Fourier integrals over 2π period can be replaced by finite sums according to any numerical method for integral evaluation. For periodic functions the Bessel formulae are recommended. In such a case, a_1 and b_1 can be approximated by:

$$a_1 = \frac{1}{N}\sum_{k=0}^{2N-1} I_k \cos\frac{k\pi}{N},$$

$$b_1 = \frac{1}{N}\sum_{k=0}^{2N-1} I_k \sin\frac{k\pi}{N} \tag{3}$$

where I_k are the exit intensity distributions observed with bias $\Phi_B = \Phi_k = k\pi/N$, and $2N$ is the number of equidistant points Φ_k, where the intensity samples are taken. They have to run over the entire periods of I, so that $I(\Phi_0) = I(\Phi_{2N})$.

With the number of samples $2N = 4$ the phase of interest can be retrieved from

$$\Delta(x,y) = \arctan\left[\frac{I_1(x,y)-I_3(x,y)}{I_0(x,y)-I_2(x,y)}\right] \tag{4}$$

where I_0, I_1, I_2 and I_3 are the intensity distributions as observed with $\Phi_B = 0, \pi/2, \pi, 3\pi/2$, respectively. It means that by introducing a $\pi/2$ step in the bias Φ_B, the phase function $\Delta(x,y)$ at every point of the image plane can be unequivocally reconstructed from four interferograms taken in each phase step.

Suppose that the basic interference formula (1) describes the interference pattern as observed is a transverse wavefront shearing microinterferometer, where a phase object is investigated. When the wavefront shear exceeds object dimensions, two separate images can be observed and the function

$$\Gamma(x,y) = (\lambda/2\pi)\Delta(x,y) \tag{5}$$

represents the optical path length through the object. If the shear is very small, then $(\lambda/2\pi)\Delta(x,y)$ is proportional to the derivative of the optical path length $\Gamma(x,y)$ in the shear direction, where the image shear s is the proportionality constant (see, for example, ref. [11])

$$\frac{d\Gamma}{dy} = \frac{1}{s}\frac{\lambda}{2\pi}\Delta(x,y). \tag{6}$$

In this case, the object is said to be observed in a differential interference contrast (DIC).

In each case, the optical path length $\Gamma(x,y)$ through the object can be either directly obtained or numerically reconstructed from the phase data $\Delta(x,y)$ retrieved from four intensity distribution measurements as required by formula (4). In the case of optically homogeneous phase objects, the optical path length is a product of the object refractive index and its transversal dimension (*i.e.*, along the optical axis) and can be directly used to retrieve any of these parameters.

3. Experimental set-up

We propose to implement the technique described above in a well-known Pluta microscope commercialized by the Polish Optical Works as Biolar PI. It is a biological microscope with dia illumination, equipped with a polarized-light interference head. The interferometer principle of this instrument is based on the shearing properties of the Wollaston prism. Thanks to different configurations of the Wollaston prism(s) and objective focus, the fringe interferograms as well as homogeneous field (infinite width fringe) interferograms can be obtained with variable image shear. No modifications are necessary to use this instrument as a phase-stepping device.

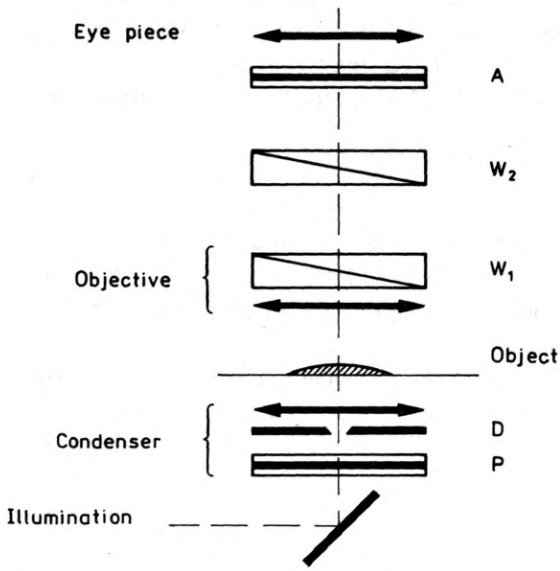

Fig. 1. Optical scheme of the microinterferometer Biolar MPI: P – polarizer, D – regulable slit diaphragm, W_1 – rotatable Wollaston prism, W_2 – tube Wollaston prism (with posibility of horizontal and vertical translation), A – analyser

The microscope is shown schematically in Figure 1. Its basic elements are two Wollaston prisms W_1 and W_2. The first is located in the objective, closely behind its optical system and is rotatable about optical axis. The second one is placed in the microscope tube and can be translated both in parallel and perpendicular direction to the axis. The system incorporates also a slit condenser diaphragm to assure illumination coherence in direction of the image shear, a polarizer placed before the condenser, and an analyser behind the second prism. The commercially available Biolar PI is equipped with three interchangeable tube prisms. Two of them are used to obtain uniform interference with large and differential image shear. The third one gives rise to the fringe interference with high image shear. Additional set of objectives with objective Wollaston prisms is also provided. The objective prisms do not influence the character of the interference observed, but the final image shear depends on the respective positions of both prisms used.

The homogeneous field interference is obtained when the fringe localization plane of the tube Wollaston prism is situated in the vicinity of the focal plane of the objective. Very wide interference fringes are formed in the image plane, which result in practically homogeneous interference in the limited field of view of the microscope. The quasi-constant bias Φ_B depends on the lateral position of the prism and is 0 when the prism is centered on the optical axis of the microscope. The prism position is controlled by a micrometric screw. This configuration was used to implement the phase-stepping technique in applications described in the following section, and the phase steps were introduced by translating the tube prism from its central position.

The step length was determined separately for each experiment as a quarter of the interference fringe width. The fringe width was measured as a prism translation between two consecutive minima of the interference image intensity. For each microscope alignment, a step calibration is necessary because the vertical movement of the prism causes significant changes of the fringe width.

The image shears are given by the manufacturer for each tube prism, but when objective prism is employed the image shear has to be measured for each experiment separately.

Incoherent illumination was used (the halogen bulb illuminator provided by the microscope manufacturer) and an interference filter was applied assuring monochromatic light of $\lambda = 0.59$ μm – about the maximum of sensibility of the image capting camera.

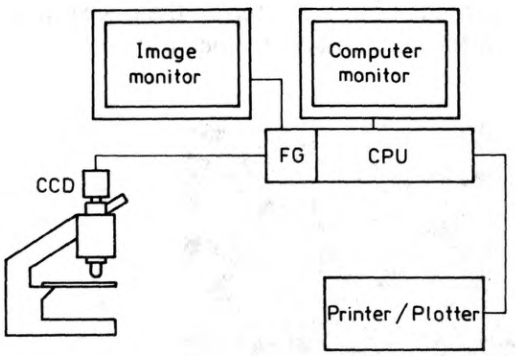

Fig. 2. Experimental set-up: CCD – the image capting CCD camera, FG – PC based frame grabber, CPU – host computer processing unit

The microscope was directly coupled to the image processing system via a CCD camera (Fig. 2). The total field of view and the instrument resolution are limited by the camera sensor dimensions and single pixel dimensions, respectively. With 10× microscope objective the total field of view was 256×358 μm and resolution was 0.5 and 0.7 μm in respective directions (due to nonsquare pixel shape).

All experimental data was extracted and processed by a PC/AT compatible computer with Data Translation DT 2851 image processing board (frame grabber) of 512×512 pixels. Basing on the subroutine library operating the board, special software was elaborated that performs the image processing as well as the necessary data acquisition and reduction. All numerical calculus was carried out by the central processing unit of the host computer. As was pointed out by ROSVOLD [12], there is a possibility of accelerating data reduction by direct use of the frame grabber arithmetic logic unit and pixel brightness mapping functions (lock-up tables), but the accuracy of this procedure is too low for most microinterferometric purposes. In general, the best solution is to use the floating point array processors, but unfortunately, it is also the most expensive one.

4. Application to surface profiling of photoresist surface: example of differential data extraction

In many areas of electronics and optoelectronics, the photoresist impressed patterns are used. In fabrication of electronic integrated circuits, photoresist masks are indispensable and the profile of their slopes is an important parameter. For optical holographic elements, such as zone plates, the surface profile is essential for their efficiency. Up to now, the most common tool for profiling of such elements were mechanical profilometers. Their use has two disadvantages: first, mechanical damage of the element under investigation is possible, and second, the profile can be taken from one line only in each measurement and many scans are necessary for surface mapping. On the other hand, the low reflectance of such surfaces makes it very difficult to use optical microscopic profilers working in reflected light.

We propose to use the phase-stepping technique implemented in the microinterferometer described in the preceding section to take surface profiles of transparent

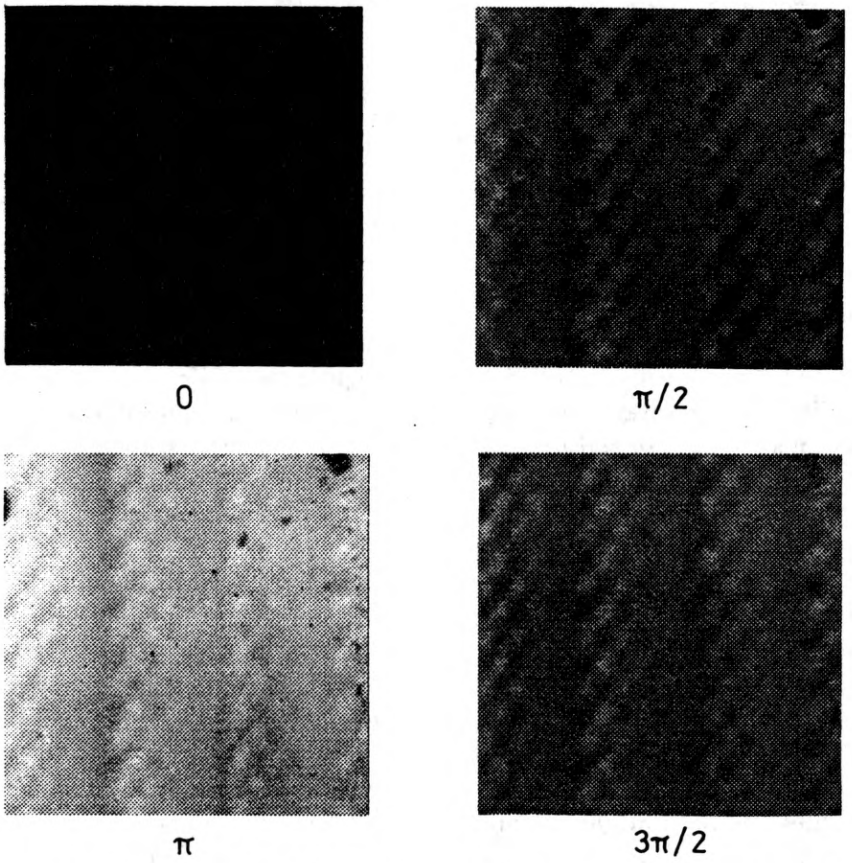

Fig. 3. Four homogeneous field interferograms of a photoresist impressed zone plate with the phase bias Φ_B of $0\pi/2$, π, and $3\pi/2$, respectively. The horizontal image shear in the object plane was 1.35 μm

objects over the whole field of view of the instrument and with the advantage of working in transmitted light.

In Figure 3, four homogeneous field interferograms of a zone plate fabricated in photoresist are shown. They correspond to the constant phase bias Φ_B of 0, $\pi/2$, π, and $2\pi/3$, respectively, and were obtained by placing the tube Wollaston prism of small shear in the objective focus and conveniently displacing it three times in the direction perpendicular to the system axis. The total image shear was equal to 1.35 μm (in the object plane), so the phase data obtained from Eq. (4) was considered differential. This data was numerically integrated to obtain the optical path length at each point. Assuming constant refractive index of the photoresist, the optical path length was expressed as a product of its refractive index and thickness:

$$\Gamma(x,y) = nd(y,x). \tag{7}$$

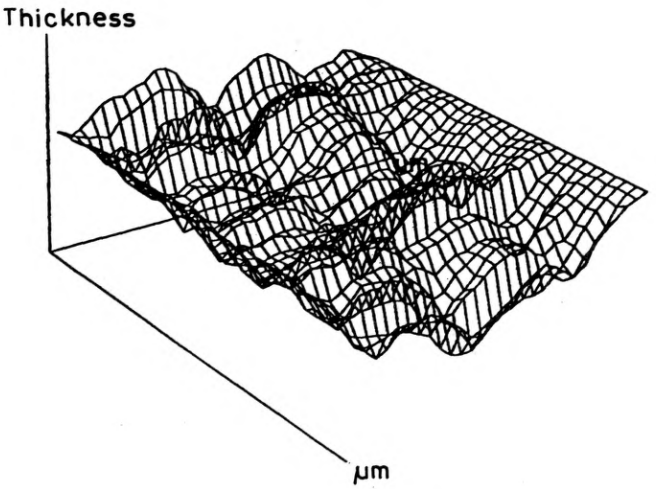

Fig. 4. Surface map of the zone plate of Fig. 3

The results of thickness extraction are plotted as a surface map in Fig. 4, where the resist thickness at each point is given with respect to the medium thickness in each scan line. The axes of this plot were arbitrarily rescaled to bring the surface shape into relief. The fine structure of the object can be easily appreciated together with the expected periodic structure of zones. This granular fine structure is a result of the fabrication process in which a photographically reduced mask was used, previously prepared in a computer laser printer. The optical density of the master-mask was controlled by the printer points density and diameter, causing residual granularity of the final product.

To compare the results given by our method with those of a classical diamond stylus profilometer (TALYSTEP – an instrument fabricated by Rank Tylor Hobson Ltd.), a mechanically scratched photoresist surface was investigated. Figure 5**a** shows the map of a fragment of the sample, and in Fig. 5**b**, the single scan profiles obtained

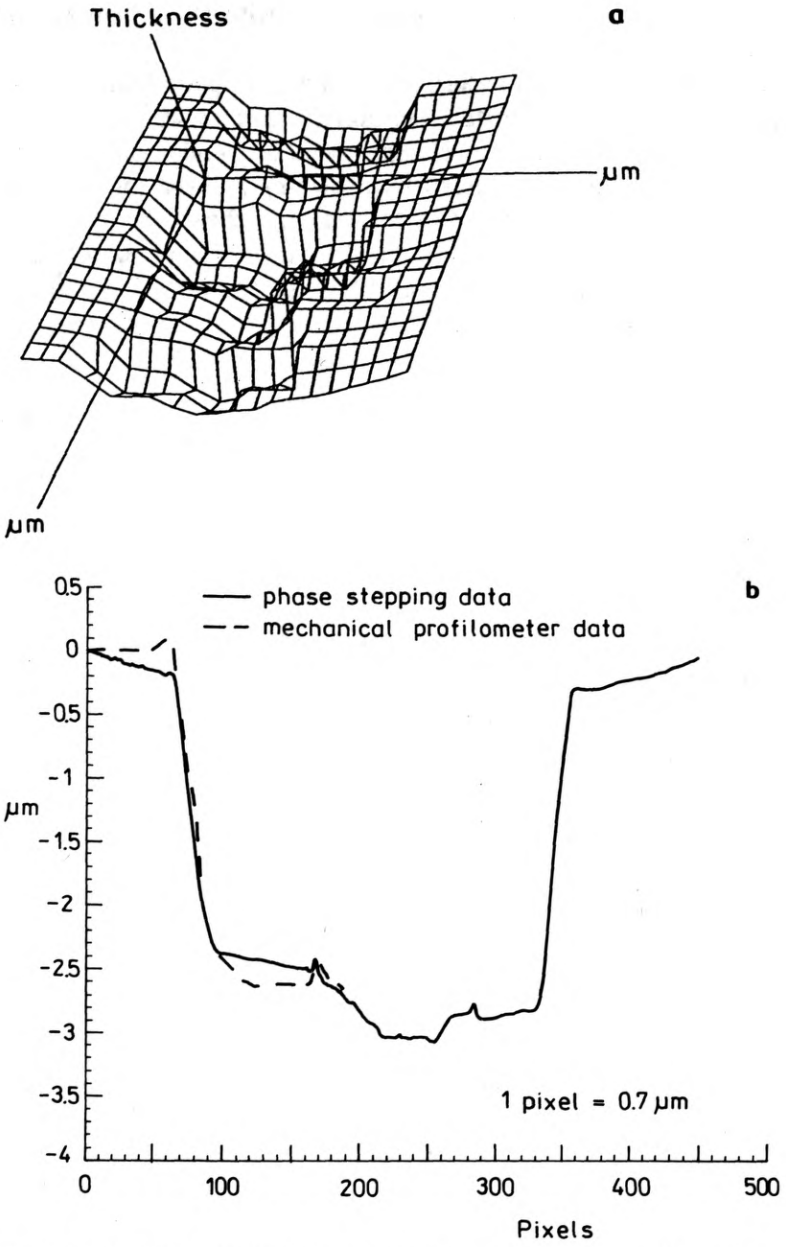

Fig. 5. Mechanically scratched photoresist layer: a — surface map retrieved from phase-stepping data, and b — single line profile compared with that taken with a diamond stylus

by both methods can be compared. The map of Fig. 5a is equivalent to 100 profile lines 358 μm long separated by 0.5 μm from each other. The system used is capable of data acquisition for up to 512 profile lines.

Finally, a sinusoidal profile zone plate was measured. Its surface plot is shown in Fig. 6a, and in Fig. 6b a single line profile can be compared with the one obtained by

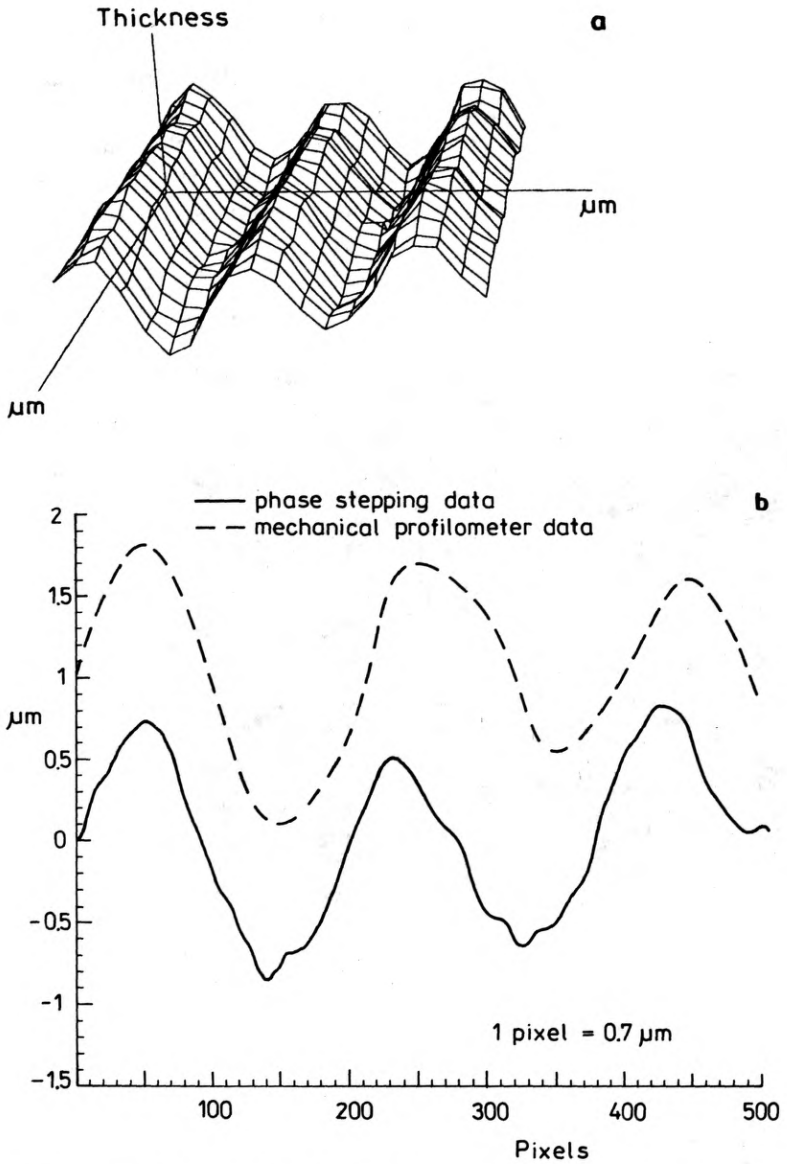

Fig. 6. Sinusoidal zone plate fabricated in photoresist: **a** — surface map obtained by phase-stepping interferometry, and **b** — single line profile compared with that of a diamond stylus profilometer

a mechanical profilometer. The relative smoothness of the stylus scan in comparison with the PSI profile can be attributed to the high stylus speed at data acquisition.

In both cases, the scan area was identified by a stylus mark made intentionally at the sample edge. The precision of the stylus trace identification is estimated in few micrometers. This repositioning error is surely the reason of small differences between the thickness profiles of Fig. 5**b**.

5. Application to abrupt steps evaluation in a transparent optical coating: example of direct phase data extraction

When the object under study is an abrupt edge of a dielectric layer, for example, a thin optical coating, the differential interference contrast is of little or no use at all, as the phase derivative at the very edge tends to infinity and, at the same time, extremely small image shears are required to assure the shear smaller than the object, *i.e.* edge, transversal dimension. Large image shear should be applied in such cases and direct phase measurements carried out.

In an experimental set-up described above, with a tube prism of high shear used together with objective prism in additive position, the total image shear of

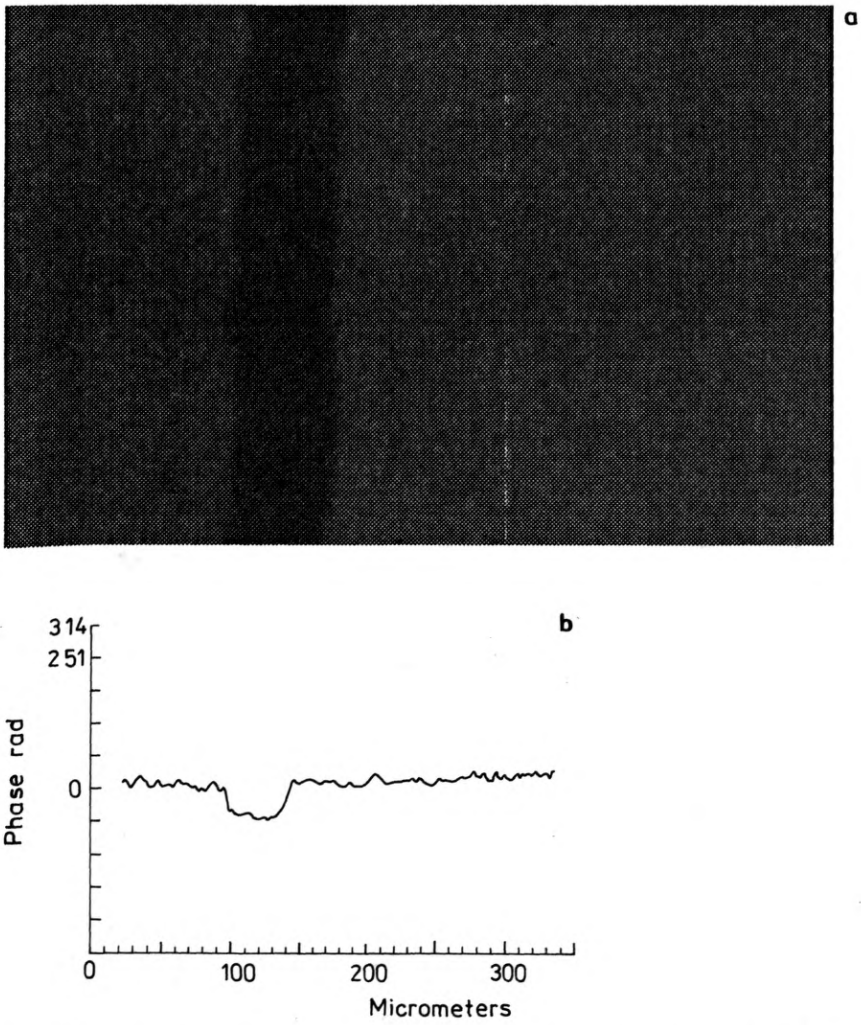

Fig. 7. Dielectric layer step: **a** — one of four homogeneous field interferograms taken with the image shear of 44.5 μm, and **b** — phase difference between sheared image parts retrieved from a single line scan

44.5 μm was obtained. Using the same light wavelength and illumination conditions as in the preceding part, various objects were investigated such as thin optical coatings, very small glass wedges and optical waveguides.

In Figure 7**a**, a fragment of one of the four homogeneous field interferograms of an abrupt edge of a thin optical coating (F_2Cr) is shown. Two edge images can be easily seen. In each interferogram, the light intensity depends on the optical path length difference between two superposed parts of the sample. It is the same in the left and right parts of each interferogram, where no path difference exists, and is different in its central part, where the image of the substrate is superposed with the image of coated glass. In Figure 7**b**, a single horizontal scan of retrieved and 2π unwrapped phase is shown.

Phase data obtained in this experiment were used in the film deposition control.

6. Accuracy considerations

The systematic error sources in classical phase retrieving interferometers have been analysed by several authors [3], [13]–[15]. Three main error sources are recognized: that of the bias Φ_B determination, the influence of extraneous light, and the coherent noise. The influence of each type of errors on the final result depends on the algorithm used in the phase extraction. The dependence of the phase measurement errors due to the phase-shifter miscalibration and to the detector nonlinearity on algorithm was studied exhaustively by CREATH [3].

The extraneous light and the coherent noise are of less or no importance in microinterferometry because small numerical apertures are usually used as well as incoherent illumination sources. The most important source of errors for the implementation described remains the error of determining the bias Φ_B for each step as well as random errors of this phase. Their analysis, as given by SCHWIDER *et al.* [13], is also valid in the case of Wollaston prism phase shifter. In the experimental set-up described in preceding sections, the single step determination precision was about 1.53% in differential interference contrast and 4.65% in total image shearing, which, according to Schwider, should result in the mean value of phase error of the order of 0.02 rad and 0.07 rad, respectively.

Finally, the phase measurement precision is limited by the interference image contrast according to the relation

$$\delta\Delta = \frac{2\pi}{N} \tag{8}$$

where N is the image contrast expressed in the grey levels of the digitizing device. In the best case, N is equal to the whole range of the digitizer grey levels. When an 8 bit digitizing device is used, 256 grey levels images are processed. In this case, the phase measurement precision $\delta\Delta = 0.02$ rad is attained. It can be easily seen that the phase measurement precision limit due to the image contrast is of the same order of magnitude as errors due to the phase-shifter error or greater.

As the phase is calculated separately at each point, spatial illumination homo-

geneity is of no importance. It is not so with temporal stability of illumination and this parameter should be monitored during data acquisition. It has, however, an easy solution: in the case where illumination stability secured by the intsrument is not sufficient it is possible to compensate for it by appropriate software. The manual control of the camera gain is indispensable.

When working with a differential interference contrast, proper attention should also be paid to the precision in the image shear determination. For some configurations it is a constant parameter, given by the producer, however, in many cases it has to be measured during the experiment.

6. Conclusions

In spite of requirements mentioned above the phase-stepping technique has proved an efficient method of data acquisition for the dielectric film surface profiling in transmitted light. The speed and precision are much higher than for the diamond stylus profiling and the advantage of nondestructivity is obvious. The implementation proposed is a direct one and does not require any modifications of the instrument used. It can also be used with other wavefront shearing microinterferometers, providing the interference bias is a controllable parameter. What is more, the possibility to use variable image shear makes the implementation described a very versatile one. Depending on the object properties, the user is free to extract phase data proportional to the optical path length or its derivative. This choice can be also subject to the information required as a final result.

Finally, it should be pointed out that applications described above have rather exemplary character. There exist numerous possible applications of phase-stepping in microscopy of transparent objects. The most interesting seem to be the refractive index profiling of microlenses and other inhomogeneous objects such as optical waveguides, phase diffraction gratings, *etc.*, as well as precise quantitative measurements in biomedicine.

Acknowledgements – Sincere appreciation is felt to Vicente Moreno, Maria Jesus Mendez and Manuel Ulibarrena for providing numerous samples and profilometer results.

The first author wishes to extend her thanks to the Spanish Ministry of Education and Xunta de Galicia for financial support as well as to the University of Santiago for their hospitality. The second author acknowledges the COMET grant that enabled him to take part in this work.

References

[1] BRUNING J. H., HERRIOTT D. R., GALLAGHER J. E., ROSENFELD D. P., WHITE A. D., BRANGACCIO D. J., Appl. Opt. 13 (1974), 2693.

[2] SCHWIDER J., *Advanced evaluation techniques in interferometry*, [In] *Progress in Optics*, Vol. XXVIII, [Ed.] E. Wolf, 1990, p. 271.

[3] KUJAWIŃSKA M., *Automatic fringe pattern analysis in optical methods of testing*, [In] Prace Naukowe–Mechanika, Zeszyt 138, [Ed.] Warsaw Technical University, 1990.

[4] CREATH K., *Phase-measurement interferometry techniques*, [In] *Progress in Optics*, Vol. XXVI, [Ed.] E. Wolf, 1988, p. 349.

[5] SA BUT L., PATORSKI K., KUJAWIŃSKA M., Opt. Eng. 31 (1992), 422.

[6] MORALES A., CREATH K., *Contact and noncontact profilers*, [In] *Optical Shop Testing*, 2nd edition., [Ed.] D. Malacara, Wiley 1992.
[7] *Microscope use phase shifting interferometry*, Opt. Laser Technol. **23** (1991), 261.
[8] WYANT J. C., SPIE **525** (1985), 174.
[9] CREATH K., SPIE **661** (1986), 296.
[10] SHIMADA W., SATO T., YATAGAI T., SPIE **1332** (1990), 525.
[11] PLUTA M., *Advanced Light Microscopy*, Vol. 2, PWN (Polish Scientific Publishers)—Elsevier, Amsterdam 1989.
[12] ROSVOLD G. O., Appl. Opt. **29** (1990), 237.
[13] SCHWIDER J., BURROW R., ELSSNER K.—E., GRZANNA J., SPOLACZYK R., MERKEL K., Appl. Opt. **22** (1983), 3421.
[14] KINNSTAETTER K., LOHMAN A. W., SCHWIDER J., STREIBL N., Appl. Opt. **27** (1988), 5082.
[15] LAI G., YATAGAI T., J. Opt. Soc. Am. **8** (1991), 822.

Received December 2, 1993